

CHAPTER 4.

Turbulence Modelling	4 - 1
4.1 A Hierarchy of Turbulence Models	4 - 1
4.1.1 Second-Order Closure	4 - 2
4.1.2 Algebraic Stress Models	4 - 6
4.1.3 Eddy-Viscosity Models	4 - 9
4.2 Modifications to the Standard k - ϵ Model	4 - 12
4.2.1 Low-Reynolds-Number k - ϵ Models	4 - 12
4.2.2 Non-Linear k - ϵ Models	4 - 15
4.2.3 Streamline Curvature Modification	4 - 18
4.2.4 Preferential Response of Dissipation to Normal Strains	4 - 22
4.3 Near-Wall Modelling By Wall Functions	4 - 24

CHAPTER 4.

Turbulence Modelling

4.1 A Hierarchy of Turbulence Models

For many pressure-dominated flows a comparatively simple turbulence model suffices if one requires only the mean field and pressure force coefficients. For example, linearised models of flow over low hills (Jackson and Hunt, 1975; Taylor et al., 1983) have achieved remarkably high mileage from a mixing-length description of turbulence in the inner layer, whilst Euler flow calculations are regularly used for airfoil sections. By contrast, major impetus for improving turbulence models has come from areas where the turbulent transport of a scalar is of paramount importance - for example, heat transfer and pollution dispersion.

Direct numerical simulation of turbulence is not an option for any but the lowest Reynolds number flows, although it has recently come to be used for the testing and calibrating of various models and revealing the nature of, for example, near-wall turbulence and laminar-to-turbulent flow transition. For most applications the choice of turbulence models lies somewhere in the hierarchy depicted in Figure 4.1, with a preponderance of activity at the second-order closure and (one- or two-equation) eddy-viscosity levels. In principle, the more elevated position in the hierarchy the more general the turbulence model, but, since each step on the ladder demands substantially greater computational effort, there comes a point where the increase in cost exceeds available resources or outweighs any potential benefits arising from an increase in accuracy or generality. The computational effort required for geometrically complex three-dimensional flows is sufficiently large for us to concentrate our efforts on tailoring simpler eddy-viscosity models to the particular flows of interest and Sections below will describe modifications to the standard k - ϵ model to accommodate effects of mean-streamline curvature, alongwind pressure gradients and, in the next Chapter, a limiting length scale. However, to set the scene and to highlight effects which are not amenable to treatment with an isotropic eddy-viscosity model we shall first review more general statistical closures.

4.1.1 Second-Order Closure

Second-order closure is rapidly becoming accepted as the frontline regiment in the regular army of turbulence models (Hanjalic, 1994) to the extent that the UMIST "basic model" (Launder, 1989) has become established as a standard framework in the same way as the Launder and Spalding (1974) k - ϵ model for two-equation eddy-viscosity models. In second-order closure transport equations are solved for the individual turbulent fluxes of momentum, $\overline{u'_i u'_j}$, and scalars, $\overline{\theta' u'_i}$, which appear in the mean-flow equations. To define notation and identify processes, the (exact) transport equations for these fluxes, together with the turbulent kinetic energy, $k = 1/2 \overline{q^2} = 1/2 \overline{u'_i u'_i}$, and scalar fluctuations, $\overline{\theta^2}$, are set out below.

<u>advection</u>	<u>production</u>	<u>pressure</u> <u>-strain</u>	<u>diffusion</u>	<u>dissipation</u>	
$\frac{D}{Dt} \overline{u'_i u'_j}$	$-\left(\overline{u'_i u'_k} \frac{\partial U_j}{\partial x_k} + \overline{u'_j u'_k} \frac{\partial U_i}{\partial x_k} \right) + \overline{(f'_i u'_j + f'_j u'_i)}$	$+\frac{\overline{p'}}{\rho} \left(\frac{\partial u'_i}{\partial x_j} + \frac{\partial u'_j}{\partial x_i} \right)$	$+\frac{\partial}{\partial x_k} \left[-\frac{\overline{p'}}{\rho} (u'_i \delta_{jk} + u'_j \delta_{ik}) + \nu \frac{\partial}{\partial x_k} (\overline{u'_i u'_j} - \overline{u'_i u'_j u'_k}) \right]$	$-2\nu \frac{\partial u'_i}{\partial x_k} \frac{\partial u'_j}{\partial x_k}$	
	P_{ij}	F_{ij}	Φ_{ij}	e_{ij}	
$\frac{D}{Dt} \left(\frac{1}{2} \overline{q^2} \right)$	$-\overline{u'_i u'_j} \frac{\partial U_i}{\partial x_j}$	$+\overline{f'_i u'_i}$	$+\frac{\partial}{\partial x_j} \left[-\frac{\overline{p' u'_j}}{\rho} + \nu \frac{\partial}{\partial x_j} \left(\frac{1}{2} \overline{q^2} \right) - \frac{1}{2} \overline{q^2 u'_j} \right]$	$-\nu \left(\frac{\partial u'_i}{\partial x_j} \right)^2$	
	P	F	D	ϵ	
$\frac{D}{Dt} \overline{(\theta' u'_i)}$	$-(\overline{\theta' u'_j} \frac{\partial U_i}{\partial x_j} + \overline{u'_i u'_j} \frac{\partial \theta}{\partial x_j})$	$+\overline{f'_i \theta'}$	$+\frac{\overline{p' \theta'}}{\rho} \frac{\partial \theta}{\partial x_i}$	$+\frac{\partial}{\partial x_j} \left[-\frac{\overline{p' \theta'}}{\rho} \delta_{ij} + \nu \theta' \frac{\partial u'_i}{\partial x_j} + \kappa u'_i \frac{\partial \theta'}{\partial x_j} - \overline{\theta' u'_i u'_j} \right]$	$-(\nu + \kappa) \frac{\partial \theta'}{\partial x_j} \frac{\partial u'_i}{\partial x_j}$
	$P_{\theta i}^{(U)} + F_{\theta i}^{(\theta)}$	$F_{\theta i}$	$\Phi_{\theta i}$	$D_{\theta i}$	
$\frac{D}{Dt} \left(\frac{1}{2} \overline{\theta^2} \right)$	$-\overline{\theta' u'_i} \frac{\partial \theta}{\partial x_i}$		$+\frac{\partial}{\partial x_j} \left[\kappa \frac{\partial}{\partial x_j} \left(\frac{1}{2} \overline{\theta^2} \right) - \frac{1}{2} \overline{\theta^2 u'_j} \right]$	$-\kappa \left(\frac{\partial \theta'}{\partial x_j} \right)^2$	
	P_{θ}		D_{θ}	e_{θ}	

At second-order closure level the advection and production terms are exact, but the pressure-strain, diffusion and dissipation terms must be modelled. Turbulent fluxes derive their energy from the mean flow (and body forces) via the production terms and lose it ultimately to heat via viscous dissipation. Between source and sink the stresses may be advected, diffused and

the energy redistributed between components, mainly by the action of pressure forces in the pressure-strain or "return-to-isotropy" term. To explain this appellation, observe that the pressure-strain contributions for the normal stresses $\overline{u'^2}$, $\overline{v'^2}$, $\overline{w'^2}$ are $2\frac{p'}{\rho}\frac{\partial u'}{\partial x}$, $2\frac{p'}{\rho}\frac{\partial v'}{\partial y}$ and $2\frac{p'}{\rho}\frac{\partial w'}{\partial z}$ respectively. These sum to zero (by continuity) and it is generally accepted that their action is to attempt to bring about an equipartition of energy amongst the individual components. The modelling of the pressure-strain interaction is crucial to second-order closure schemes.

The divergence of the Navier-Stokes equation yields a Poisson equation for the pressure. Given the velocity field, this may be solved by standard methods to obtain the pressure field as a sum of a volume integral over the flow domain plus a surface integral over its boundary. Extracting the fluctuating part, it can be shown (Launder, 1989) that the pressure-strain may be written as a sum of:

- (i) a term involving products of the turbulent fluctuations only;
- (ii) a term containing products of Reynolds stresses and mean-velocity gradients;
- (iii) a term involving body forces.

Each term is further subdivided into a volume integral plus a surface integral determining the effect of boundaries. Given this decomposition, and the assumption that the pressure-strain promotes a return to isotropy, a typical expression for the pressure-strain has the following form:

$$\Phi_{ij} = \Phi_{ij}^{(u)} + \Phi_{ij}^{(P)} + \Phi_{ij}^{(F)} + \Phi_{ij}^{(wall)} \quad (4.1)$$

where

$$\begin{aligned} \Phi_{ij}^{(u)} &= -C_1 \frac{\epsilon}{k} \overline{(u'_i u'_j)}^* \\ \Phi_{ij}^{(P)} &= -C_2 P_{ij}^* \\ \Phi_{ij}^{(F)} &= -C_3 F_{ij}^* \\ \Phi_{ij}^{(wall)} &= [C'_1 \frac{\epsilon}{k} \overline{u'_k u'_l} + C'_2 \Phi_{kl}^{(P)} + C'_3 \Phi_{kl}^{(F)}] n_k (\delta_{ij} n_l - \frac{3}{2} \delta_{il} n_j - \frac{3}{2} \delta_{jl} n_i) f(\frac{l_e}{\kappa l_n}) \\ &(C_1=1.8, \quad C_2=C_3=0.6, \quad C'_1=0.5, \quad C'_2=0.3, \quad C'_3=0) \end{aligned} \quad (4.2)$$

and a superscript * denotes the deviatoric (ie, traceless) part: $T_{ij}^* = T_{ij} - \frac{1}{3} T_{kk} \delta_{ij}$. In the wall term,

l_ϵ is the dissipation length and l_n the normal distance from the wall. A similar form is projected for the "pressure-scrambling" terms in the scalar-flux equations:

$$\Phi_{\theta i} = \Phi_{\theta i}^{(u)} + \Phi_{\theta i}^{(P)} + \Phi_{\theta i}^{(F)} + \Phi_{\theta i}^{(wall)} \quad (4.3)$$

where

$$\begin{aligned} \Phi_{\theta i}^{(u)} &= -C_{\theta 1} \frac{\epsilon}{k} \overline{\theta' u'_i} \\ \Phi_{\theta i}^{(P)} &= -C_{\theta 2} P_{i\theta}^{(U)} \\ \Phi_{\theta i}^{(F)} &= -C_{\theta 3} F_{i\theta} \\ \Phi_{\theta i}^{(wall)} &= [C'_{\theta 1} \frac{\epsilon}{k} \overline{\theta' u'_j} + C'_{\theta 2} \Phi_{j\theta}^{(P)} + C'_{\theta 3} \Phi_{j\theta}^{(F)}] n_j n_i f(\frac{l_\epsilon}{\kappa l_n}) \\ &(C_{\theta 1}=2.9, \quad C_{\theta 2}=C_{\theta 3}=0.4, \quad C'_{\theta 1}=0.25, \quad C'_{\theta 2}=C'_{\theta 3}=0) \end{aligned} \quad (4.4)$$

For the calibration of the various constants one is referred to Launder's paper.

The "wall" part of the pressure-strain contains the distance to the wall, l_n , and it is the difficulty of specifying this normal distance for corrugated or otherwise complex boundaries which has resulted in much recent work to reformulate the pressure-strain model in such a way as to remove this troublesome term. Advances in this direction, together with attempts to satisfy, for example, *realisability* (in particular, the positivity of normal stresses) and the two-dimensional limit (which is approached near a wall), have been described in Launder (1989).

The remaining terms to be parameterised are the diffusion and dissipation parts. As can be seen from the stress-transport equations, the first typically comprises pressure diffusion, (molecular) gradient diffusion and third-order correlations. These may be modelled independently (Hanjalic, 1994). The dissipation term represents the ultimate sink of turbulent energy and is usually assumed isotropic:

$$\epsilon_{ij} = \frac{2}{3} \epsilon \delta_{ij}, \quad \epsilon_{\theta i} = 0 \quad (4.5)$$

If, in addition, we assume the ratio of turbulent timescales, $R = \frac{1/2 \overline{\theta'^2} / \epsilon_\theta}{k/\epsilon}$, to be unity, then the

system of equations is closed by the specification of ϵ . This may be accomplished either directly through a modelled transport equation, or via a dissipation length l_ϵ such that

$$\epsilon = \frac{u_0^3}{l_\epsilon} \quad (4.6)$$

where u_0 is a typical velocity-fluctuation magnitude. l_ϵ may be specified directly on geometrical grounds or derived from a transport equation (eg, Mellor and Yamada, 1982). Most of the common parameterisations involved in second-order closure tacitly assume that all length scales are proportional to the dissipation length. An example demonstrating that this proportionality does not hold in general is given in Chapter 5.

The principal advantage of second-order closure is its capacity to deal with strong anisotropy, where individual stress components are selectively enhanced. This may be ascribed to the fact that the production terms are exact and do not need modelling. Anisotropic forcing is of particular importance in flows with body forces. Two examples arise in the atmospheric context - buoyancy and Coriolis forces.

For buoyancy forces driven by variations in a non-passive scalar θ we have (with gravitational acceleration $\bar{\mathbf{g}}$ in the negative z direction):

$$f'_i \equiv -\frac{\rho' \bar{g}}{\rho_a} \delta_{i3} = \alpha g \theta' \delta_{i3} \quad (4.7)$$

where $\alpha = -\frac{1}{\rho} \left(\frac{\partial \rho}{\partial \theta} \right)_p$ is the coefficient of expansion. Hence

$$\overline{f'_i u'_j} = \alpha g \overline{\theta' u'_j} \delta_{i3}, \quad \overline{f'_i \theta'} = \alpha g \overline{\theta'^2} \delta_{i3} \quad (4.8)$$

Thus, buoyancy forces inject turbulence energy selectively into (or remove energy from) the vertical velocity fluctuations $\overline{w'^2}$ and vertical scalar flux $\overline{\theta' w'}$.

A similar anisotropic forcing occurs in a rotating frame where there are fluctuating Coriolis forces

$$f'_i = -2\epsilon_{ilm}\Omega_l u'_m \quad (4.9)$$

so that, with $\bar{\Omega}$ aligned with the z axis),

$$\overline{f'_i u'_j} = 2\Omega\epsilon_{im3}\overline{u'_m u'_j}, \quad \overline{f'_i u'_i} = 0 \quad (4.10)$$

Thus, there are equal and opposite contributions $4\Omega\overline{u'v'}$ and $-4\Omega\overline{u'v'}$ to the $\overline{u'^2}$ and $\overline{v'^2}$ budgets respectively - an effect which cannot be predicted with an isotropic eddy-viscosity model, since the net contribution to the turbulent kinetic energy is zero.

In complex three-dimensional flows, second-order closure models are expensive - transport equations for six stress components, three scalar fluxes (per variable), dissipation ϵ and scalar fluctuations. Various rational attempts to simplify them have been proposed - for example, the hierarchy of turbulence models for geophysical flow problems of Mellor and Yamada (1974, 1982), based on classifying terms according to their degree of anisotropy, and the partly related route of algebraic stress modelling, to which we shall now turn.

4.1.2 Algebraic Stress Models

Algebraic stress models represent an attempt to reduce the computational effort of full second-order closure whilst retaining the effects of anisotropic forcing. They are based on the premise that the rate of change of the structure function $\overline{u'_i u'_j}/k$ is considerably less than that of the turbulent kinetic energy itself; that is:

$$\left(\frac{D}{Dt} - \mathit{diff}\right)\overline{u'_i u'_j} \approx \frac{\overline{u'_i u'_j}}{k} \left(\frac{D}{Dt} - \mathit{diff}\right)k = \frac{\overline{u'_i u'_j}}{k}(P+F-\epsilon) \quad (4.11)$$

(where " diff " stands for the diffusion term). With this simplification, the full Reynolds-stress equations (excluding, for simplicity, the wall terms in the pressure-strain, (4.1)) reduce to the algebraic equations

$$\overline{\frac{u'_i u'_j}{k}} - \frac{2}{3} \delta_{ij} = \frac{\Phi}{\epsilon} (\Pi_{ij} - \frac{2}{3} \delta_{ij} \Pi) \quad (4.12)$$

where

$$\Phi = \frac{1-C_2}{C_1+\gamma}, \quad \gamma = \frac{\Pi}{\epsilon} - 1 \quad (4.13)$$

Here, $\Pi_{ij}=P_{ij}+F_{ij}$ is the total production term. Dissipation is taken to be isotropic: $\epsilon_{ij}=\frac{2}{3}\epsilon\delta_{ij}$. We have assumed that $C_2=C_3$ and it is also common to assume local equilibrium ($\gamma=0$). Neither assumption is strictly necessary.

A similar simplification may be postulated for the scalar fluxes:

$$\left(\frac{D}{Dt} - diff\right) \overline{\theta' u'_i} \approx \frac{\overline{\theta' u'_i}}{\sqrt{k(\nu_2 \theta'^2)}} \left(\frac{D}{Dt} - diff\right) \sqrt{k(\nu_2 \theta'^2)} = \nu_2 \overline{\theta' u'_i} \left(\frac{\Pi - \epsilon}{k} + \frac{P_\theta - \epsilon_\theta}{\nu_2 \theta'^2}\right) \quad (4.14)$$

Substitution into the transport equations yields

$$\overline{\theta' u'_i} = \Phi_T \frac{k}{\epsilon} P_{\theta i}^{(\Theta)} + \Phi_T' \frac{k}{\epsilon} (P_{\theta i}^{(U)} + G_{\theta i}) \quad (4.15)$$

where

$$\Phi_T = \frac{1}{C_{\theta 1} + \gamma_\theta}, \quad \gamma_\theta = \frac{1}{2} \left[\left(\frac{\Pi}{\epsilon} - 1 \right) + \frac{1}{R} \left(\frac{P_\theta}{\epsilon_\theta} - 1 \right) \right] \quad (4.16)$$

$$\Phi_T' = (1 - C_{\theta 2}) \Phi_T$$

R is the ratio of turbulent timescales. Again, we have assumed $C_{\theta 2}=C_{\theta 3}$, whilst it is common to assume local equilibrium ($\gamma_\theta=0$).

Equations (4.12) and (4.15) relate the turbulent fluxes to the production terms in such a way as to retain the *local* anisotropy of forcing (as expressed through the production terms) but without the *history* of anisotropy (as expressed by the advection terms). Thus, in a rather simplistic fashion we can summarise the various levels of modelling in Table 4.1 below.

	Anisotropy of forcing	History of anisotropy
Reynolds-stress model	Yes	Yes
Algebraic stress model	Yes	No
Eddy-viscosity model	No	No

Table 4.1: Handling of anisotropy in various turbulence model closures.

At first sight, replacing six stress-transport equations by a single transport equation for k , plus algebraic relations for the structure functions $\overline{u_i u_j}/k$, might be perceived as an excellent means of incorporating anisotropic processes without substantial cost. At the bottom line, however, one still requires storage space and matrix solution algorithms for the $\overline{u_i u_j}$, so that we have discarded the generality of second-order closure without gaining much in return. As an additional warning, neither the conventional pressure-strain formulation in the full Reynolds-stress closure, nor the algebraic stress equation (4.12) ensure realisability; in particular, that each normal stress be positive.

Examination of the Table above might prompt one to wonder if eddy-viscosity models can have any part to play in flows where anisotropy is known to assume a major role. The answer is a resounding "yes" and the reason is simple: in many flows only one component of the stress may be significant. This is particularly true if we are only interested in the mean flow. If an eddy-viscosity model can be tailored to yield satisfactory values for this stress term in the regions of the flow where it is significant then we have a useful model. Although apparently little used in their own right, algebraic stress models have been found very useful in indicating modifications to simpler models (such as k - ϵ) to accommodate anisotropic processes such as buoyancy (Gibson and Launder, 1976; Rodi, 1985) and mean-streamline curvature (Leschziner and Rodi, 1981).

4.1.3 Eddy-Viscosity Models

By analogy with the molecular-viscosity law for Newtonian fluids, eddy-viscosity models assume a linear relation between the (deviatoric) turbulent stress tensor and the mean rate of strain via a (kinematic) *eddy viscosity*, ν_t :

$$\tau_{ij} \equiv -(\overline{u'_i u'_j} - \frac{2}{3} k \delta_{ij}) = \nu_t \left(\frac{\partial U_i}{\partial x_j} + \frac{\partial U_j}{\partial x_i} \right) \quad (4.17)$$

and between the turbulent scalar fluxes and mean gradients via a turbulent Prandtl number, σ_θ :

$$-\overline{\theta' u'_i} = \frac{\nu_t}{\sigma_\theta} \frac{\partial \theta}{\partial x_i} \quad (4.18)$$

As with any other diffusivity, the eddy viscosity has dimensions of [velocity]×[length], and this motivates its modelling. Physically, the velocity scale, u_0 , should be proportional to the magnitude of the turbulent perturbation, whilst the length scale, l_m , is representative of the distance a fluid particle may move whilst retaining its dynamical properties. The four commonest forms of model are as follows (simplest first).

- (i) *Eddy viscosity specified directly*. For example, in the atmospheric surface layer (see Section 5.2):

$$\nu_t = \frac{\kappa u_* z}{\phi_M(z/L_{MO})} \quad (4.19)$$

where u_* is the friction velocity, L_{MO} is the Monin-Obukhov length and ϕ_M is a stability-dependent function taking a value of unity in uniform density flow. (These variables will be defined more precisely in Chapter 5.)

- (ii) *Mixing-length models*. The velocity scale is taken as the change in mean velocity over a (specified) mixing length, l_m ; ie, $u_0 = l_m \frac{\partial U}{\partial z}$, or, in a tensorially invariant form, $u_0 = l_m S$, where $S = \sqrt{2S_{ij}S_{ij}}$ is the mean-strain invariant and $S_{ij} = \frac{1}{2} \left(\frac{\partial U_i}{\partial x_j} + \frac{\partial U_j}{\partial x_i} \right)$ is the rate-of-strain tensor. The turbulent stress is given by

$$-\overline{(u'_i u'_j - \frac{2}{3} k \delta_{ij})} = 2l_m^2 S S_{ij} \quad (4.20)$$

which reduces, in a simple shear flow, to

$$-\overline{u'w'} = l_m^2 \left| \frac{\partial U}{\partial z} \right| \frac{\partial U}{\partial z} \quad (4.21)$$

- (iii) *One-equation models.* Typically, $v_t \propto k^{1/2} l_m$, where the length scale is specified algebraically (usually on geometric grounds) and a transport equation is solved for the turbulent kinetic energy k . In the atmospheric boundary layer, for example,

$$\frac{1}{l_m} = \frac{1}{\kappa z} + \frac{1}{l_{max}} \quad (4.22)$$

where κz is the eddy size determined by the distance from the surface and l_{max} is some maximum mixing length, determined, for example, by stratification or the depth of the boundary layer. The transport equation for k will be given below.

- (iv) *Two-equation models.* Typically, transport equations for the turbulent kinetic energy k and either a length scale or a derived scale. In the widely used k - ϵ turbulence model the second transport equation is that for the dissipation rate ϵ and we have:

$$\begin{aligned} \text{velocity scale:} \quad u_0 &= C_\mu^{1/4} k^{1/2} \\ \text{length scale:} \quad l_m &= l_\epsilon \equiv \frac{u_0^3}{\epsilon} \end{aligned} \quad (4.23)$$

giving an eddy viscosity

$$v_t = C_\mu \frac{k^2}{\epsilon} \quad (4.24)$$

(The separation of constants between velocity and length scales is somewhat arbitrary: the above choice is made for reasons of consistency.) Note that there is only one length scale. Modelled transport equations are solved for k and ϵ :

$$\begin{aligned}\frac{Dk}{Dt} &= \frac{\partial}{\partial x_j} \left[\left(v + \frac{v_t}{\sigma_k} \right) \frac{\partial k}{\partial x_j} \right] + \Pi - \epsilon \\ \frac{D\epsilon}{Dt} &= \frac{\partial}{\partial x_j} \left[\left(v + \frac{v_t}{\sigma_\epsilon} \right) \frac{\partial \epsilon}{\partial x_j} \right] + (C_{\epsilon 1} \Pi - C_{\epsilon 2} \epsilon) \frac{1}{\tau_\epsilon}, \quad \tau_\epsilon = \frac{k}{\epsilon}\end{aligned}\tag{4.25}$$

where Π is the overall production rate of turbulent kinetic energy, the sum of terms P and F due to shear and (in this application) buoyancy forces respectively:

$$\begin{aligned}P &\equiv -\overline{u_i' u_j'} \frac{\partial U_i}{\partial x_j} = v_t \left(\frac{\partial U_i}{\partial x_j} + \frac{\partial U_j}{\partial x_i} \right) \frac{\partial U_i}{\partial x_j} \\ F &\equiv \alpha g \overline{w' \theta'} = -\alpha g \frac{v_t}{\sigma_\theta} \frac{\partial \Theta}{\partial z}\end{aligned}\tag{4.26}$$

Unless specified otherwise the applications described in this Thesis use the constants

$$C_\mu = 0.09, \quad C_{\epsilon 1} = 1.44, \quad C_{\epsilon 2} = 1.92, \quad \sigma_k = 1.0, \quad \sigma_\epsilon = 1.11, \quad \sigma_\theta = 0.9\tag{4.27}$$

With the exception of σ_ϵ these are the values recommended by Launder and Spalding (1974). σ_ϵ was chosen to make the model consistent with the constant-flux, surface-layer similarity profiles characterised by a logarithmic velocity profile (in uniform density flow):

$$C_{\epsilon 2} - C_{\epsilon 1} = \frac{\kappa^2}{\sigma_\epsilon \sqrt{C_\mu}}\tag{4.28}$$

The model is most sensitive to C_μ , which sets the general level of turbulence, and the difference $C_{\epsilon 2} - C_{\epsilon 1}$, since this determines the balance of production and removal terms in the dissipation equation and hence the length scale. In principle, C_μ can be determined from the structure constant $(\tau/k)^2$, which implies $C_\mu = 0.033$ for rough-wall boundary layers (Raithby et al., 1987). We have retained the more conventional value $C_\mu = 0.09$, based on Klebanoff's original smooth-walled flat-plate data, since the set of constants were originally optimised *in toto* and changes in C_μ should not be undertaken without re-optimising $C_{\epsilon 1}$ and $C_{\epsilon 2}$.

4.2 Modifications to the Standard k - ϵ Model

Hanjalic (1994) and others have identified major deficiencies of two-equation eddy-viscosity models. They include the inability of a linear stress-strain relationship based upon a single isotropic eddy viscosity to cope with, for example:

- history of anisotropy; eg, wake flows;
- anisotropic body forces; eg buoyancy, Coriolis forces;
- complex strains; eg, curved flows, alongwind pressure gradients;
- viscous effects in low-Reynolds-number and transitional flows;
- non-equilibrium flow near walls;
- flows with more than one length or time scale.

Whilst second-order closure can overcome the first three problems, the latter three still remain and the modelling of the pressure-strain interaction creates new difficulties. Numerically, Reynolds-stress transport models are computationally intensive and notoriously unstable. By contrast, eddy-viscosity models are readily incorporated into existing laminar viscous codes through a stability-enhancing addition to the implicit diffusion term. There is, therefore, widespread appeal for the idea of "tweaking" eddy-viscosity models for particular types of flow.

This Section will review briefly two particular types of extended two-equation closures - low-Reynolds-number and non-linear k - ϵ models - and then examine, in some detail, two k - ϵ modifications which have been coded in SWIFT to account for complex strains - mean-streamline curvature and streamwise pressure gradients. In Chapter 5 a novel "limited-length-scale k - ϵ model" is proposed for flows where the turbulent mixing length is limited by some external constraint.

4.2.1 Low-Reynolds-Number k - ϵ Models

Numerical practices for modelling turbulent shear flows near walls divide sharply into two camps - low-Reynolds-number turbulence models designed to resolve the flow right down to

the viscosity-dominated sublayer and wall-function approaches which bridge the gap between a node lying in the fully turbulent region and the wall with some well-defined universal profiles. Since atmospheric flows are inherently of high Reynolds number (and the surface is aerodynamically rough) the wall-function approach is invariably used for such simulations and this technique will be described in Section 4.3. However, for code validation against small-scale flows in the laboratory, integration right to the wall using a low-Reynolds-number model may be desirable.

The requirement for an accurate prediction of flow separation and laminar/turbulent transition means that near-wall modelling is important in many engineering flows. However, the overriding importance of the near-wall region in thermal diffusion has inevitably meant that much of the impetus for refining both modelling practices has come from the heat-transfer research community. Indeed, it was the difficulty of obtaining direct experimental measurements in the vicinity of the wall that led Chieng and Launder (1980) to suggest that heat-transfer comparisons were perhaps the best means of assessing the near-wall modelling of turbulence. This has all changed with the availability of detailed direct numerical simulation (DNS) data (eg, Rodi, 1993) and it is inevitable that much more model calibration will be carried out in future through this medium.

A large number of low-Reynolds-number k - ϵ models appear in the literature. A representative sample consists of the models of Launder and Sharma (1974), Lam and Bremhorst (1981), Chien (1982) and Lien and Leschziner (1993). Other examples can be found in the review of Patel et al. (1985) and the work of Rodi and Mansour (1993). A common formulation for such models has been given by Patel et al. (1985). The direct effects of molecular viscosity on the shear stress and turbulent length scale are incorporated by the inclusion of *damping factors* in the eddy-viscosity formulation and the dissipation equation; thus:

$$v_t = C_{\mu} f_{\mu} \frac{k^2}{\tilde{\epsilon}} \quad (4.29)$$

$$\frac{D\tilde{\epsilon}}{Dt} = \frac{\partial}{\partial x_j} \left[\left(v + \frac{v_t}{\sigma_e} \right) \frac{\partial \tilde{\epsilon}}{\partial x_j} \right] + (C_{\epsilon 1} f_1 \mathbf{P} - C_{\epsilon 2} f_2 \tilde{\epsilon}) \frac{\tilde{\epsilon}}{k} + E \quad (4.30)$$

Some models (eg, Launder and Sharma, 1974, and Chien, 1982) choose to solve for the dissipation variable

$$\tilde{\epsilon} = \epsilon - D \quad (4.31)$$

where D asymptotes to the correct value of dissipation as the wall is approached ($\epsilon \sim 2\nu k/l_n^2, k \propto l_n^2$ - see Patel et al., 1985), in order to apply the convenient numerical boundary condition $\tilde{\epsilon}=0$ at the surface. f_μ, f_1 and f_2 are, typically, functions of the non-dimensional combinations

$$\begin{aligned} l_n^+ &= \frac{u_\tau l_n}{\nu} \\ l_n^* &= \frac{\sqrt{k} l_n}{\nu} \\ R_t &= \frac{k^2}{\nu \epsilon} \end{aligned} \quad (4.32)$$

where l_n is the normal distance from the wall. The damping factors, plus the additional terms D and E , are given for the four representative low-Reynolds-number models in Table 4.2.

For the practical motivation behind each model one should refer to the original papers, but, in general, f_2 is chosen to reflect the change with Reynolds number of the exponent in the decay law of isotropic turbulence, f_1 or E to return the correct behaviour of dissipation near the wall, and f_μ to incorporate the transition from turbulent to viscous momentum transport as the wall is approached. Note that Lien and Leschziner's model is an attempt to effect a smooth transition from the two-equation k - ϵ model to a one-equation model (l_m and l_ϵ specified) in the viscous sublayer.

To resolve the viscous sublayer the nearest grid node must be at an l_n^+ value of order unity.

Model	f_μ	f_1	f_2	D	E
Launder and Sharma (1974)	$e^{-\frac{3.4}{(1+R/50)^2}}$	1	$1-0.3e^{-R_t^2}$	$2\nu\left(\frac{\partial k^{1/2}}{\partial x_i}\right)^2$	$2\nu\nu_t\left(\frac{\partial^2 U_i}{\partial x_j\partial x_k}\right)^2$
Lam and Bremhorst (1981)	$(1-e^{-0.0165l_n^*})^2 \times (1+\frac{20.5}{R_t})$	$1+\left(\frac{0.05}{f_\mu}\right)^3$	$1-e^{-R_t^2}$	0	0
Chien (1982)	$1-e^{-0.0115l_n}$	1	$1-0.22e^{-(R_t/6)^2}$	$\frac{2\nu k}{l_n^2}$	$-2\nu\frac{\tilde{\epsilon}}{l_n^2}e^{-0.5l_n^+}$
Lien and Leschziner (1993)	$\frac{l_n^{(1)}/l_e^{(1)} = \kappa l_n(1-e^{-0.016l_n^*})}{\kappa l_n(1-e^{-0.263l_n^*})}$	1	$1-0.3e^{-R_t^2}$	0	$C_\epsilon f_2 \frac{C_\mu^{3/4} k^{3/2}}{l_e^{(1)}} \frac{e}{k} \times e^{-l_n^{+2}/450}$

Table 4.2: Coefficients for low-Reynolds-number models.

Note: Chien uses non-standard k - ϵ constants $C_{\epsilon 1}=1.35$, $C_{\epsilon 2}=1.8$.

4.2.2 Non-Linear k - ϵ Models

For thin shear layers, the standard k - ϵ model works well because the normal Reynolds stresses do not enter into the calculation of the mean velocity. Whilst this provides an acceptable representation of the mean flow the same cannot be said for the turbulence statistics. For example, in fully-developed channel flow the standard k - ϵ model (or, indeed, any other isotropic eddy-viscosity model) predicts that the normal stresses are all equal (to $2k/3$), in flagrant contradiction of experiment. As Speziale (1987) demonstrates for fully-developed flow in non-circular ducts, in the absence of any distinction between the normal stresses, an isotropic eddy-viscosity model will fail to predict the development of the secondary (cross-

stream) circulations which are observed in experiments. It is clear that an accurate representation of the normal stresses will be equally important in curved and separated flows.

The search for a better representation of the normal Reynolds stresses without a sacrifice of the beneficial aspects of the k - ϵ model - such as its ease of application and its reduction to a mixing-length model for thin shear flows - has prompted the development of a number of *non-linear* or *anisotropic* extensions. Both appellations are widely used and equally appropriate. The anisotropic property indicates an advance over the strict proportionality between deviatoric stress and mean strain. The non-linear description refers to the derivation of models as terms in an asymptotic expansion in powers of the mean-velocity gradients, with the standard isotropic form being obtained as the linear term (Speziale, 1991). However, a modicum of caution needs to be exercised with this formal derivation, since the dimensionless expansion parameter is, effectively, $C_\mu \frac{k}{\epsilon} S$ (S a representative velocity gradient), which takes the rather moderate value 0.3 in equilibrium shear flows.

Speziale (1987) derived a model based on "material frame indifference"; that is, invariance under arbitrary (even accelerated) changes of reference frame - not just inertial transformations. (This has been criticised as too restrictive for general turbulent flow, since it only applies in the limit of two-dimensional turbulence and generally imposes a stronger constraint than is satisfied by the equations of motion themselves.) Speziale notes that terms which are quadratic in $\partial U_i / \partial x_j$ are of the same dimension as those which are linear in $D/Dt(\partial U_i / \partial x_j)$, whilst the frame-indifferent parts of these tensors are S_{ij} and $\overset{\circ}{S}_{ij}$, where

$$\overset{\circ}{S}_{ij} = \frac{DS_{ij}}{Dt} - \frac{\partial U_i}{\partial x_k} S_{kj} - \frac{\partial U_j}{\partial x_k} S_{ki} \quad (4.33)$$

is the *Oldroyd* derivative. Thus, a material-frame-indifferent model which is quadratic in the velocity gradients (and contains the standard, isotropic, eddy-viscosity model as the linear term) must take the form

$$-\left(\frac{\overline{u_i' u_j'}}{k} - \frac{2}{3} \delta_{ij} \right) = 2C_\mu \frac{k}{\epsilon} S_{ij} + 4 \left(C_\mu \frac{k}{\epsilon} \right)^2 [C_D S_{ik} S_{kj} + C_E \overset{\circ}{S}_{ij}]^* \quad (4.34)$$

where, as before, the superscript * denotes the deviatoric or traceless part. The constants c_D and c_E are calibrated with respect to measurements of the normal stresses in full-developed channel flow (where, incidentally, the advective parts $\vec{U} \cdot \nabla S_{ij}$ of the Oldroyd derivative vanish). Values $c_D \approx c_E \approx 1.68$ are adopted. Although Speziale shows (in principle) that his model is capable of predicting secondary flows in non-circular ducts, this is not unique to his scheme, but is generally true of non-linear models which are quadratic in the mean-velocity gradients.

Rubinstein and Barton (1990) describe an alternative non-linear model by extending Yakhot and Orszag's (1986) renormalisation-group (RNG) procedure, curtailing the iterative process at second order. The often-quoted advantages claimed for the RNG analysis are that all model constants emerge naturally from the theory rather than having to be calibrated, and that the theory is valid for both high and low Reynolds numbers. Rubinstein and Barton's model for the Reynolds stresses is

$$-\left(\frac{\overline{u_i' u_j'}}{k} - \frac{2}{3} \delta_{ij} \right) = 2C_\mu \frac{k}{\epsilon} S_{ij} - \left(\frac{k}{\epsilon} \right)^2 \left[C_{\tau 1} \frac{\partial U_i}{\partial x_k} \frac{\partial U_j}{\partial x_k} + C_{\tau 2} \left(\frac{\partial U_i}{\partial x_k} \frac{\partial U_k}{\partial x_j} + \frac{\partial U_j}{\partial x_k} \frac{\partial U_k}{\partial x_i} \right) + C_{\tau 3} \frac{\partial U_k}{\partial x_i} \frac{\partial U_k}{\partial x_j} \right]^* \quad (4.35)$$

where

$$C_\mu = 0.0845, \quad C_{\tau 1} = 0.034, \quad C_{\tau 2} = 0.104, \quad C_{\tau 3} = -0.014 \quad (4.36)$$

Shih et al. (1993) derived a third non-linear relationship between Reynolds stress and mean strain by considering the most general tensorially invariant combination of second order in the mean-velocity gradients, subject to the constraints of *symmetry* and *realisability*. The latter condition means, in particular, that the model must always return non-negative normal stresses, $\overline{u_\alpha^2}$, and requires that the model coefficients be functions of the mean strain, or, in dimensionless form, $\frac{k}{\epsilon} \frac{\partial U_i}{\partial x_j}$. The remaining coefficients were calibrated with respect to rotating homogeneous shear flow and backstep flow. Shih's model takes a form very similar to that of Rubinstein and Barton (4.35), but with coefficients which are functions of the stress

invariants:

$$C_\mu = \frac{0.667}{1.25 + \bar{S} + 0.9\bar{\Omega}}, \quad C_{\tau 1} = \frac{13}{1000 + \bar{S}^3}, \quad C_{\tau 2} = \frac{-4}{1000 + \bar{S}^3}, \quad C_{\tau 3} = \frac{-2}{1000 + \bar{S}^3} \quad (4.37)$$

where

$$S_{ij} = \frac{1}{2} \left(\frac{\partial U_i}{\partial x_j} + \frac{\partial U_j}{\partial x_i} \right), \quad \Omega_{ij} = \frac{1}{2} \left(\frac{\partial U_i}{\partial x_j} - \frac{\partial U_j}{\partial x_i} \right) \quad (4.38)$$

$$S = \sqrt{2S_{ij}S_{ij}}, \quad \Omega = \sqrt{2\Omega_{ij}\Omega_{ij}}, \quad \bar{S} = S \frac{k}{\epsilon}, \quad \bar{\Omega} = \Omega \frac{k}{\epsilon}$$

We turn now to two complex-strain variants of the k - ϵ model which have been investigated using SWIFT - variants to incorporate mean-streamline curvature and streamwise pressure gradients. Respectively, these embody the two main ways of modifying the standard model:

- (i) multiplying the eddy viscosity by an anisotropy-dependent factor;
- (ii) modifying the length scale (indirectly) by altering the balance of production and removal terms in the dissipation equation.

4.2.3 Streamline Curvature Modification

This modification was originally described by Leschziner and Rodi (1981) for two-dimensional flows. A more formal mathematical derivation, based on a moving system of basis vectors, allows a natural extension to three-dimensional flows.

If at some point in a flow we consider a cartesian coordinate system (x,y,z) with x *locally* in the direction of the mean wind, then *curvature* is essentially the non-vanishing of the derivative $\partial V/\partial x$ (Figure 4.2). Inspection of the full Reynolds-stress transport equations shows that this derivative makes contributions $-\overline{2u'v'} \frac{\partial V}{\partial x}$ and $-\overline{u'^2} \frac{\partial V}{\partial x}$ to the production terms of $\overline{v'^2}$ and $\overline{u'v'}$ respectively. Assuming that $\partial U/\partial y$ has the same sign as the shear stress $-\overline{u'v'}$ this means that curvature will promote stability/reduce cross-stream fluctuations if $\frac{\partial U}{\partial y} \frac{\partial V}{\partial x} < 0$ and increase turbulence if $\frac{\partial U}{\partial y} \frac{\partial V}{\partial x} > 0$.

In other words, *concave curvature* (velocity increasing towards the centre of curvature) is destabilising, whilst *convex curvature* (velocity decreasing toward the centre of curvature) is stabilising (Figure 4.3). In the case of a boundary layer perturbed by a small hump the (non-separated) flow typically goes through a sequence of concave→convex→concave curvature. Over the summit the opposing effects of convex curvature and increased shear respectively act to reduce or enhance the crosswind fluctuations.

Moreover, the argument above suggests that the effects of curvature are determined by the product $\frac{\partial U}{\partial y} \frac{\partial V}{\partial x}$ or, non-dimensionalising with a turbulent timescale, by $\left(\frac{k}{\epsilon}\right)^2 \frac{\partial U}{\partial y} \frac{\partial V}{\partial x}$. Leschziner and Rodi (1981) showed, by an algebraic stress procedure, that this was indeed the curvature-dependent term in a simple variant of the k - ϵ model. The following is a more formal reworking of their method, which also extends it naturally to three dimensions.

Given a flow field $\vec{U}(\vec{x},t)$ one can define, at any point, streamwise and normal vectors \vec{e}_s and \vec{e}_n respectively by

$$\begin{aligned}\vec{U} &= U_s \vec{e}_s \\ \frac{\partial \vec{e}_s}{\partial s} &= -\kappa_c \vec{e}_n\end{aligned}\tag{4.39}$$

κ_c is the *curvature*; (reciprocal of the radius of curvature, R_c). The directions of \vec{e}_s and \vec{e}_n (see Figure 4.2) are well-defined in a curved flow if we adopt the convention that $U_s > 0$, $\kappa_c > 0$, although this means that in a planar flow \vec{e}_n could be obtained from \vec{e}_s by either a clockwise or anticlockwise rotation through 90° .

Given some point in the flow, establish a rectangular cartesian coordinate system (x_1, x_2, x_3) which is *locally* aligned with the streamline system. Then, at that particular point,

$$\begin{aligned}\vec{e}_1 &= \vec{e}_s \\ \vec{e}_2 &= \vec{e}_n \\ \vec{e}_3 &= \vec{e}_1 \wedge \vec{e}_2\end{aligned}\tag{4.40}$$

(Note, however, that $\{\vec{e}_1, \vec{e}_2, \vec{e}_3\}$ are constant vectors, whilst \vec{e}_s and \vec{e}_n are functions of

position.) Then

$$\begin{aligned}\frac{\partial U_1}{\partial x_2} &= \frac{\partial U_s}{\partial n} \\ \frac{\partial U_2}{\partial x_1} &= -\kappa_C U_s\end{aligned}\tag{4.41}$$

To examine the effects of curvature alone we shall assume that these are the *only* non-zero velocity derivatives at this point. Application of the algebraic stress model (4.12) - a *local* model, remember - yields

$$\begin{aligned}\overline{u'^2} &= \frac{2}{3}k(1-\phi\Pi/\epsilon) + \frac{\phi k}{\epsilon}(-2\overline{u'v'})\frac{\partial U_s}{\partial n} \\ \overline{v'^2} &= \frac{2}{3}k(1-\phi\Pi/\epsilon) + \frac{\phi k}{\epsilon}(2\overline{u'v'})\kappa_C U_s \\ \overline{u'v'} &= \frac{\phi k}{\epsilon}\left(\overline{u'^2}\kappa_C U_s - \overline{v'^2}\frac{\partial U}{\partial n}\right)\end{aligned}\tag{4.42}$$

which, on eliminating the normal stresses, gives

$$-\overline{u'v'} = \frac{\frac{2}{3}\phi(1-\phi\Pi/\epsilon)}{1+4\phi^2\left(\frac{k}{\epsilon}\right)^2\frac{\partial U_s}{\partial n}\kappa_C U_s} \frac{k^2}{\epsilon} \left(\frac{\partial U_s}{\partial n} - \kappa_C U_s\right)\tag{4.43}$$

In other words,

$$\tau_{12} = C'_\mu \frac{k^2}{\epsilon} \left(\frac{\partial U_1}{\partial x_2} + \frac{\partial U_2}{\partial x_1}\right)\tag{4.44}$$

where

$$C'_\mu = \frac{C_{\mu 0}}{1+4\phi^2\left(\frac{k}{\epsilon}\right)^2\frac{\partial U_s}{\partial n}\kappa_C U_s}, \quad C_{\mu 0} = \frac{2}{3}\phi(1-\phi\Pi/\epsilon)\tag{4.45}$$

(4.44) is the standard k - ϵ eddy-viscosity-model expression for the proportionality between shear stress and mean rate of strain, but with C'_μ replacing C_μ . Since it is the factor multiplying $C_{\mu 0}$ in (4.45) which embodies curvature effects, we shall use this expression to

modify the k - ϵ model, but for consistency we shall retain the more conventional value $C_{\mu 0}=0.09$, rather than that derived from the pressure-strain coefficient ϕ .

Note that the curvature-dependent factor can also be written

$$\frac{C'_{\mu}}{C_{\mu 0}} = \frac{1}{1 - 4\phi^2 \left(\frac{k}{\epsilon}\right)^2 \frac{\partial U}{\partial y} \frac{\partial V}{\partial x}} \quad (4.46)$$

in the local cartesian system. Thus, as argued earlier, positive and negative values of the dimensionless combination $\left(\frac{k}{\epsilon}\right)^2 \frac{\partial U}{\partial y} \frac{\partial V}{\partial x}$ respectively enhance or diminish cross-stream turbulent transport of momentum. Leschziner and Rodi (1981) obtain the slightly different expression

$$C'_{\mu} = \frac{C_{\mu 0}}{1 + 4\phi^2 \left(\frac{k}{\epsilon}\right)^2 \left(\frac{\partial U_s}{\partial n} + \kappa_C U_s\right) \kappa_C U_s} \quad (4.47)$$

The difference may be traced to the Reynolds-stress production terms, P_{ij} . In Leschziner and Rodi's paper these are supplemented by "pseudogeneration" terms which occur in the stress-transport equations in (s,n) coordinates. However, these are actually part of the advection term, arising as a consequence of coordinate rotation.

Although the curvature modification is most naturally depicted in two dimensions, definition (4.39) allows κ_C and $\partial U_s / \partial n$ to be evaluated in fully three-dimensional flows. \vec{e}_s is the unit vector in the direction of the local velocity. Since

$$\vec{U} \cdot \nabla \vec{U} = U_s^2 \frac{\partial \vec{e}_s}{\partial s} + \frac{\partial U_s}{\partial s} \vec{U} \quad (4.48)$$

then $-\kappa_C U_s^2 \vec{e}_n$ is simply the component of the advective acceleration ($\vec{A} = \vec{U} \cdot \nabla \vec{U}$) normal to \vec{U} . Finally,

$$\frac{\partial U_s}{\partial n} = \frac{\partial U_1}{\partial x_2} = \vec{e}_2 \cdot \nabla (\vec{U} \cdot \vec{e}_1) = s_i n_j \frac{\partial U_i}{\partial x_j} \quad (4.49)$$

where $\vec{e}_s \equiv (s_i)$, $\vec{e}_n \equiv (n_i)$.

This streamline-curvature modification will be evaluated in Chapter 6 when we consider (neutrally stable) boundary-layer flow over a two-dimensional hill. To identify the regions of stabilising and destabilising curvature we have plotted as an example in Figure 4.4 contours of the curvature-dependent factor (4.45).

In a similar fashion to that used above, Gibson and Launder (1976) simplified the algebraic stress model (4.12) and (4.15) to deduce a *buoyancy* extension of the k - ε model for a horizontal free-shear layer. Rodi (1985) generalised their work to thin shear layers parallel to a plane wall or free surface. As with the curvature modification this led to a buoyancy-dependent factor in C_μ and, in this case, the turbulent Prandtl number σ_θ . The assumptions underlying that theory - namely, unidirectional flow with velocity and density shear only normal to the flow direction - are far too restrictive to give the model much prospect of generality and its applications have been confined to vertical and horizontal buoyant jets. The dynamical similarity between curved and buoyant flows has been discussed by Bradshaw (1969).

4.2.4 Preferential Response of Dissipation to Normal Strains

Just as curvature could be identified with the non-vanishing of derivative $\partial V/\partial x$ in a cartesian coordinate system locally aligned with the flow, so the presence of an alongwind acceleration/deceleration or streamwise pressure gradient is formally represented by non-zero $\partial U/\partial x$.

Experiments demonstrate that dissipative decay of turbulence is enhanced in regions of strong favourable or adverse pressure gradients - for example, grid turbulence passed through a contraction or decelerated boundary layers respectively. In the latter case, predicted dissipation

is too small, and hence turbulence levels too large, resulting in failure to predict flow separation. Similarly, unphysical levels of turbulence are predicted upwind of bluff bodies, particularly the favourable pressure gradient near the upwind corner, enhancing momentum transport across the separated shear layer and so leading to early reattachment.

Hanjalic and Launder (1980) concluded that streamwise strains are more effective than simple shear in promoting transfer of energy from large to small scales, so enhancing the dissipation rate, and proposed increasing the source term in the dissipation equation for normal strains. This idea of a *preferential response of dissipation to normal strains* was taken up by Leschziner and Rodi (1981) whose model for the production term in the dissipation equation can be invoked as an option in SWIFT:

$$P_\epsilon = [C'_{\epsilon 1} P - C''_{\epsilon 1} v_t (2S_{ns})^2] \frac{\epsilon}{k} \quad (4.50)$$

where S_{ns} is the "shear strain", $\frac{1}{2} \left(\frac{\partial U_1}{\partial x_2} + \frac{\partial U_2}{\partial x_1} \right)$ in a rectangular coordinate system aligned so that the x_1 -axis lies in the direction of the local velocity vector. In three-dimensional flows x_2 is not well-defined and the most appropriate direction is that of the component of ∇U_1 normal to \vec{e}_1 ; ie, $\nabla U_1 - (\vec{e}_1 \cdot \nabla U_1) \vec{e}_1$.

In order that the modified dissipation equation should reduce to the standard form in a simple shear flow ($\partial U/\partial y$ the only non-zero derivative) it is necessary that the new constants satisfy

$$C'_{\epsilon 1} - C''_{\epsilon 1} = C_{\epsilon 1} \quad (4.51)$$

Following Leschziner and Rodi (1981) the values $C'_{\epsilon 1}=2.24$, $C''_{\epsilon 1}=0.8$ have been used here.

This variant of the k - ϵ model was also evaluated with respect to the Russian hill geometry in Chapter 6 and we shall have more to say about its performance there. During the development of SWIFT the code was used to compute flow over various canonical two-dimensional bluff-body configurations. The effect was to reduce turbulence upwind of, and hence the turbulent transport across, the shear layer separating from the upwind corner, increasing the length of the recirculating flow to one more consistent with experimental measurements. As an illustration, Figure 4.5 plots predicted contours of turbulent kinetic

energy with and without the dissipation modification in uniform, low-turbulence flow around a blunt rectangular plate. The effect of the modification is to suppress the unphysical levels of turbulence upstream predicted by the standard k - ϵ model (with uniform approach flow and highly favourable pressure gradient the boundary layer on the front face is laminar), restricting the generation of turbulence to the separating shear layer.

4.3 Near-Wall Modelling By Wall Functions

Low-Reynolds-number modelling has by no means supplanted wall-function approaches. This is particularly true for environmental flows where, not only is the Reynolds number very high, but the surface is aerodynamically rough, so that detailed resolution down to the wall is inconceivable. Instead, traditional wall-function approaches have been refined, particularly in complex recirculating flow where the near-wall turbulence is far from equilibrium.

For equilibrium shear flows a common assumption is a universal relationship between variables scaled on the local friction velocity u_τ . Thus

$$U^+ = f(l_n^+) \quad (4.52)$$

where

$$U^+ = \frac{U(l_n)}{u_\tau}, \quad l_n^+ = \frac{l_n u_\tau}{\nu} \quad (4.53)$$

l_n is the normal distance from the wall and $\tau_w \equiv u_\tau^2$ is the (kinematic) wall shear stress. In the fully turbulent layer:

$$U^+ = \frac{1}{\kappa} \ln(E l_n^+) \quad (4.54)$$

whilst in the viscous sublayer:

$$U^+ = l_n^+ \quad (4.55)$$

Assuming a dimensionless height l_v^+ for the viscous sublayer, matching the two profiles at this height yields

$$E = \frac{e^{\kappa l_v^+}}{l_v^+} \quad (4.56)$$

l_v^+ is usually taken to be 11.6. For strict validity, wall-function approaches require the nearest grid node to lie in the fully-turbulent region, typically in the range $30 < l_n^+ < 150$.

For rough-wall boundary layers (where individual surface elements exceed the depth of the viscous sublayer) the logarithmic velocity profile is commonly written as

$$U^+ = \frac{1}{\kappa} \ln(l_n^+/z_0) \quad (4.57)$$

where z_0 is the roughness length.

Using (4.54) or (4.57), u_τ (and hence τ_w) may be deduced from the velocity value at the near-wall node. The difficulty with scaling on the friction velocity, however, is that near stagnation points u_τ (and hence the eddy viscosity ν_t) vanish. Thus, the eddy diffusivity for heat, ν_t/σ_θ , also vanishes, whereas, in practice, the heat transfer coefficient exhibits a maximum at this point. An appropriate means of overcoming this (Chieng and Launder, 1980, based on the work of Spalding, 1967) is to use the square root of the turbulent kinetic energy, \sqrt{k} , as a velocity scale, rather than u_τ . In equilibrium flows the two formulations are equivalent since

$$u_\tau = C_\mu^{1/4} k^{1/2} \quad (4.58)$$

However, the main advantages are perceived near stagnation points, where, unlike u_τ , there is no requirement for k to go to zero.

According to Spalding (1967) the viscous sublayer thickness, l_v , adjusts itself in line with the external kinetic energy so that the sublayer Reynolds number, $l_v^* = l_v k^{1/2} / \nu$, is a universal constant with a value of ~ 20 (Launder, 1988).

In the fully turbulent layer assume an eddy-viscosity relationship for the shear stress:

$$\tau_w = \nu_t \frac{\partial U}{\partial n} \quad (4.59)$$

where, by comparison with the equilibrium case, the eddy viscosity is given by

$$\nu_t = \kappa (C_\mu^{1/4} k^{1/2}) l_n \quad (4.60)$$

Integrating for the velocity profile (with constant k and τ_w) yields

$$\frac{C_\mu^{1/4} k^{1/2} U}{\tau_w} = \frac{1}{\kappa} \ln(E^* l_n^*) \quad (4.61)$$

where $l_n^* = l_n k^{1/2} / \nu$ and, for consistency with the equilibrium case, $E^* = C_\mu^{1/4} E$.

The value of k appearing in (4.61) is k_v , the turbulent kinetic energy at the top of the viscous sublayer. Although various means have been devised to obtain this by extrapolation (eg, Chieng and Launder, 1980), the value k_p at the nearest internal node is almost always used. With the tangential velocity component U_p at the same location, (4.61) can be inverted to yield the wall shear stress

$$\tau_w = \frac{\kappa C_\mu^{1/4} k_p^{1/2} U_p}{\ln(E^* l_p^*)} \quad (4.62)$$

Numerically, this shear stress acting on the face of a control volume abutting the wall may be included explicitly (as a source term) or implicitly, via an *effective eddy viscosity* $\nu_{t,eff}$ such that

$$\tau_w = \nu_{t,eff} \frac{U_p}{l_p} \quad (4.63)$$

where

$$v_{t,eff} = \frac{\kappa C_{\mu}^{1/4} k_p^{1/2} l_p}{\ln(E^* l_p^*)} \quad (4.64)$$

A comparable treatment is available for the heat flux (Launder, 1988), but within SWIFT we have adopted the simplest procedure of using $v_{t,eff}/\sigma_{\theta}$ as an effective eddy diffusivity.

For rough-wall boundary layers an exactly similar procedure is followed, except that $E^* l_p^*$ is replaced in the logarithmic term by l_p/z_0 .

For equilibrium boundary layers, k is related to u_{τ} by (4.58) and, if u_{τ} is deduced from the velocity profile above, then this serves as a boundary condition to specify the near-wall value of k . For flows departing from equilibrium, however, it is the near-wall value of k that supplies the velocity scale and a more accurate balance of production and dissipation within the near-wall control volume is sought. *Cell-averaged* values of production and dissipation are obtained from specified profiles of U , k , ε and τ over the depth of the near-wall cell. Idealised profiles are suggested by Figure 4.6.

In the viscous sublayer, experiments suggest a linear variation in the amplitude of the fluctuating velocity component parallel to the wall, which leads to a quadratic variation in k :

$$k = k_v \left(\frac{l_n}{l_v} \right)^2 \quad (4.65)$$

As the wall is approached the diffusion of turbulent kinetic energy occurs by molecular gradient transport, which, according to this profile, vanishes at the surface. The appropriate numerical boundary condition is, therefore, no diffusion through this face.

In the viscous sublayer ε tends to a constant value ε_v (Patel et al., 1985) where

$$\varepsilon_v = \frac{2\nu k_v}{l_v^2} \quad (4.66)$$

whilst in the fully turbulent layer, where dissipation balances production:

$$\epsilon(l_n) = \frac{C_\mu^{3/4} k^{3/2}}{\kappa l_n} \quad (4.67)$$

The *cell-averaged* value of ϵ is, therefore, (assuming $k_v=k_p$):

$$\bar{\epsilon} = \frac{1}{\Delta} \int_0^\Delta \epsilon \, dl_n = \epsilon_v \frac{l_v}{\Delta} + \frac{C_\mu^{3/4} k_p^{3/2}}{\kappa \Delta} \ln(\Delta/l_v) \quad (4.68)$$

The turbulent kinetic energy production rate is given by

$$\mathbf{P} = \begin{cases} \tau_w \frac{\partial U}{\partial n} & l_n > l_v \\ 0 & l_n < l_v \end{cases} \quad (4.69)$$

and hence the cell-averaged value is

$$\bar{\mathbf{P}} = \frac{1}{\Delta} \int_0^\Delta \mathbf{P} \, dl_n = \frac{\tau_w^2}{C_\mu^{1/4} k_p^{1/2} \kappa \Delta} \ln(\Delta/l_v) \quad (4.70)$$

Equations (4.68) and (4.70) require amendment for rough-wall boundary layers where there is no viscous sublayer and the formal integration is carried out down to $l_n=z_0$. In this case,

$$\begin{aligned} \bar{\epsilon} &= \frac{C_\mu^{3/4} k_p^{3/2}}{\kappa \Delta} \ln(l_n/l_0) \\ \bar{\mathbf{P}} &= \frac{\tau_w^2}{C_\mu^{1/4} k_p^{1/2} \kappa \Delta} \ln(l_n/l_0) \end{aligned} \quad (4.71)$$

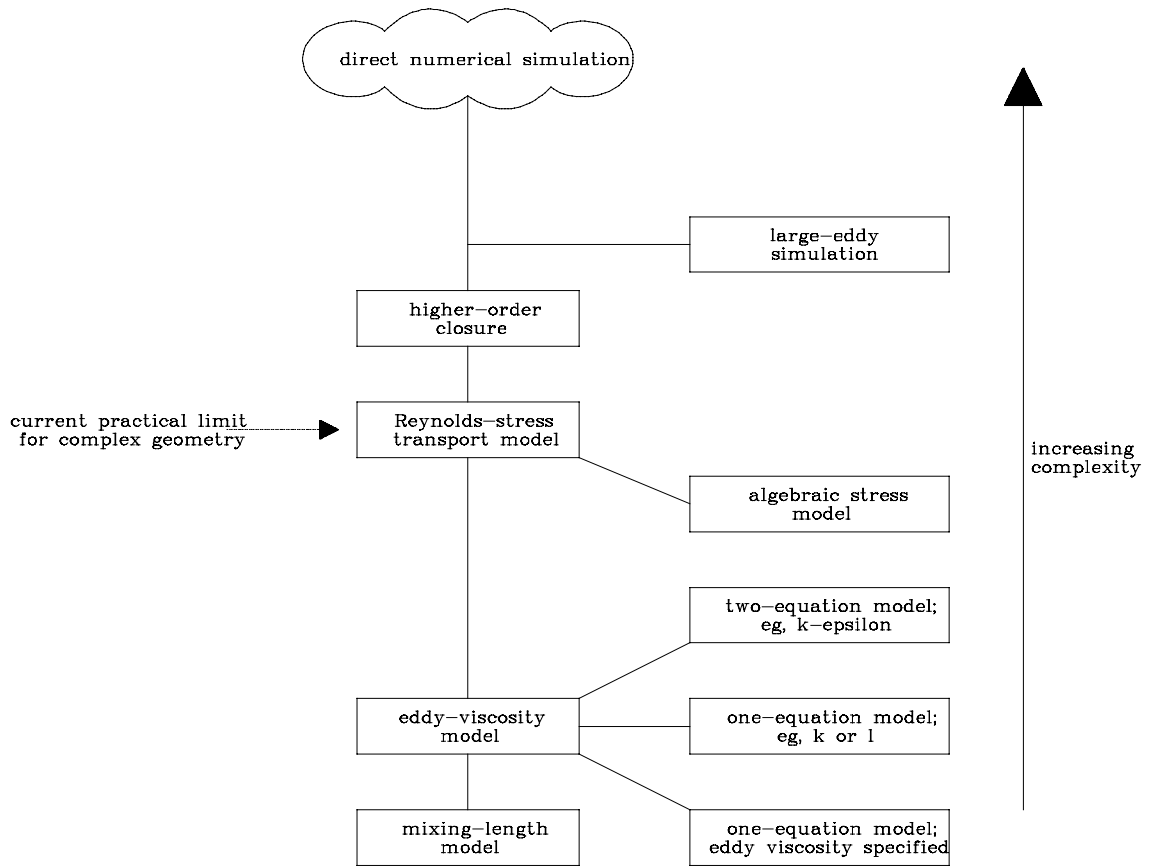


Figure 4.1: Hierarchy of turbulence models.

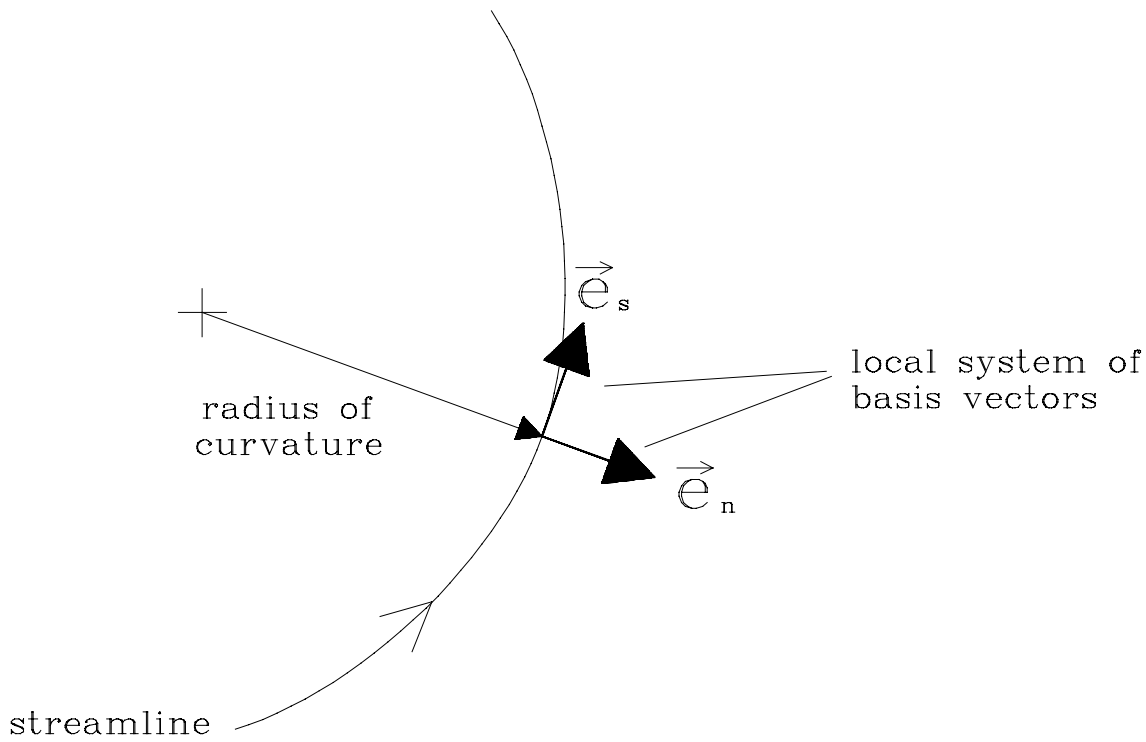


Figure 4.2: Local system of basis vectors for curved flows.

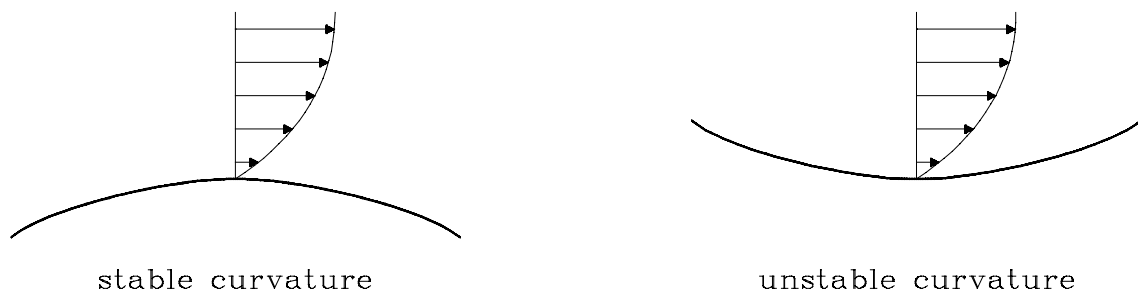


Figure 4.3: Stable and unstable curvature for boundary-layer flow.

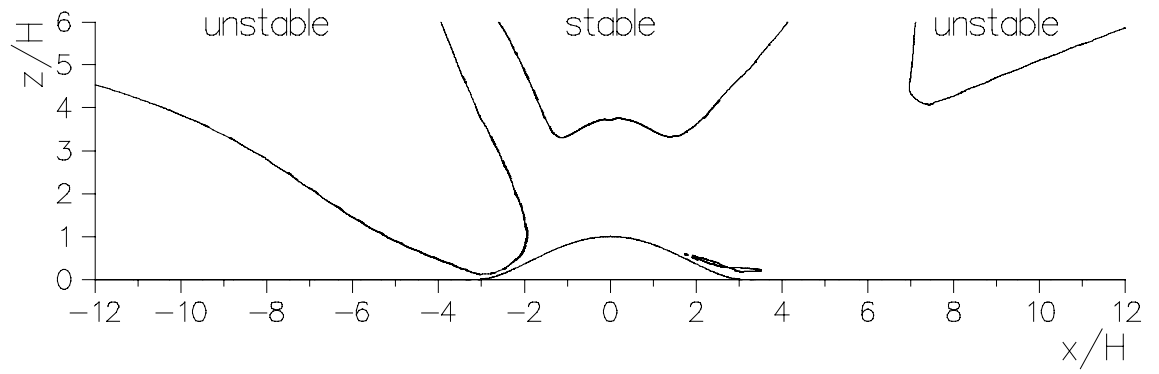
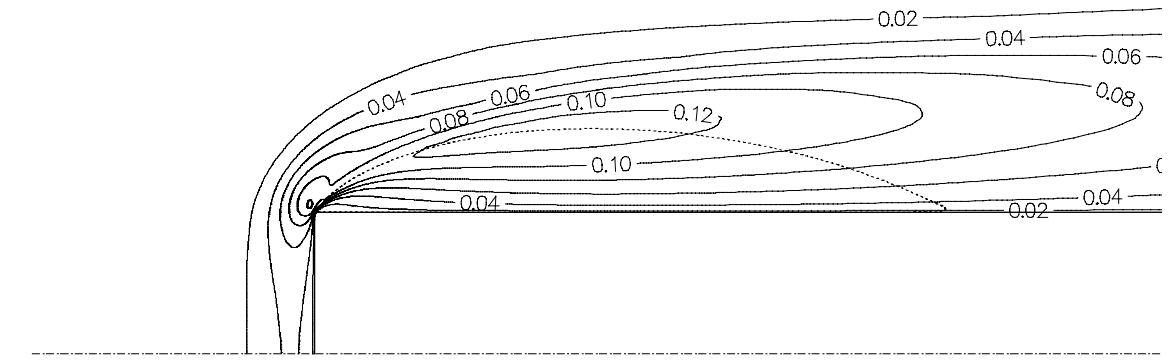
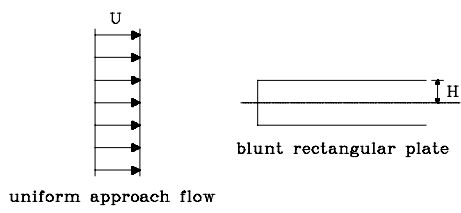
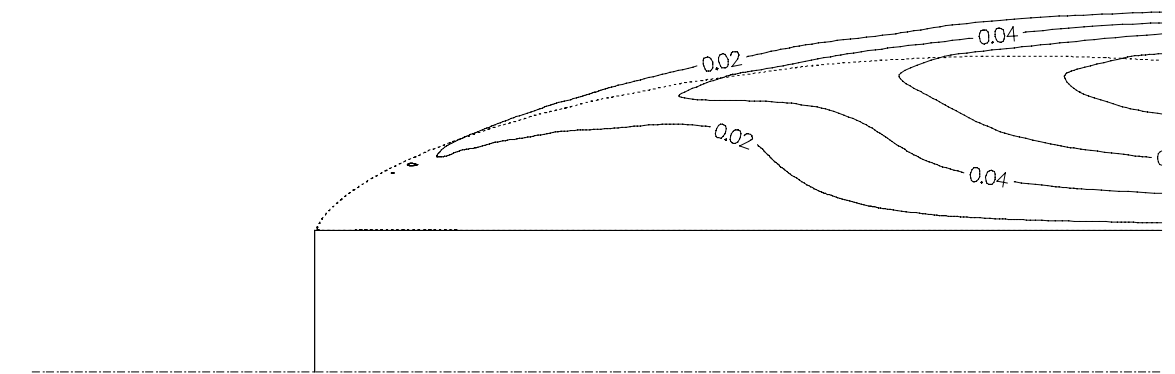


Figure 4.4: Regions of stable and unstable curvature in shear flow over a hump. Contours demark areas where the curvature-dependent factor in the eddy-viscosity expression departs from unity by more than 30%.



(a) Standard $k-\epsilon$ model



(b) With dissipation modification

Figure 4.5: Computed contours of turbulent kinetic energy (k/U_0^2) for flow around a blunt rectangular plate. The dashed line shows the separation streamline.

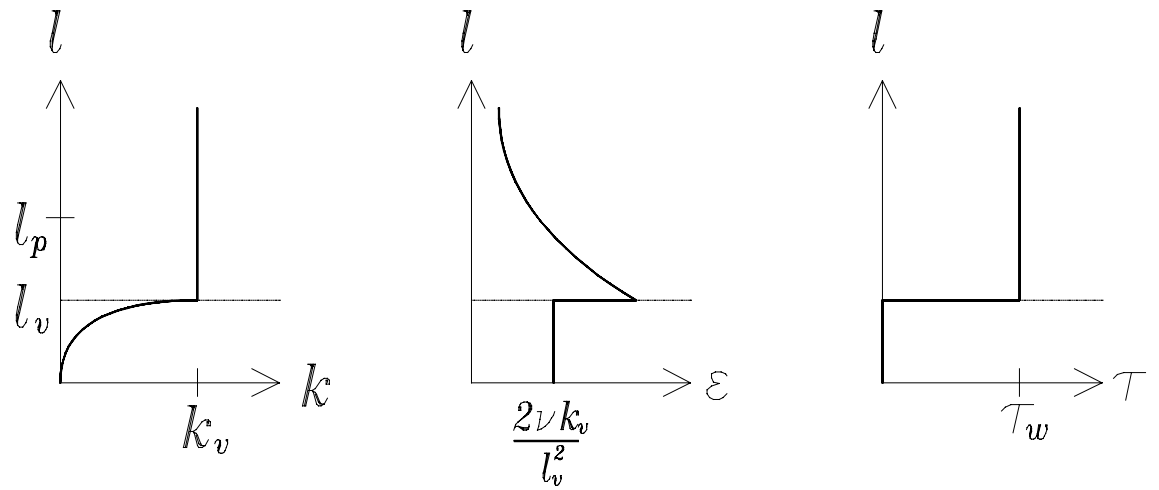


Figure 4.6: Assumed near-wall behaviour of turbulence quantities.